Global 3D acoustic FWI using sparse model parameterization

Debanjan Datta and Mrinal K. Sen, University of Texas at Austin; Scott Morton and Faqi Liu, Hess Corporation*

SUMMARY

Estimating a starting velocity model for Full Waveform Inversion can be challenging. It requires several passes of migration velocity analysis to obtain a model accurate enough to prevent cycle skipping. We present an alternative approach to estimate a 3D starting model using a global optimization method called Very Fast Simulated Annealing. To constrain the optimization problem with a large number of unknowns, we parameterize the 3D model with surfaces and velocities surrounding them and solve for the optimal parameters. The final estimated model from VFSA serves as a starting model for FWI. We demonstrate the effectiveness by comparing FWI results along a few 2D lines from the 3D model. The proposed method is largely automated and reduces numerous man hours required to build a starting model. We apply our proposed method to one toy model and one complex synthetic model. In both cases, we were able to obtain acceptable results. Use of VFSA with a sparse parameterization method makes our 3D global inversion a practical tool.

INTRODUCTION

Building a starting model for Full Waveform Inversion (Tarantola, 1984; Virieux and Operto, 2009) requires enormous man hours where an initial estimate of the velocity model is developed after multiple iterations of Migration Velocity Analysis (MVA) before arriving at a model that does not suffer from cycle skipping in the seismic bandwidth. This problem is further exacerbated in 3D where each migration pass is several orders of magnitude more expensive than that of 2D.

Several approaches have been proposed over the years to alleviate the problem of cycle skipping. The multiscale approach (Bunks et al., 1995; Sirgue and Pratt, 2004) steps over multiple frequencies to go from low to high frequencies. An alternative domain of implementation in the Laplace Fourier domain was presented by Kim et al. (2013), which focuses on different scales using damping values for the Laplace domain. Almomin et al. (2012) presented a composite objective function containing updates to both migration as well as tomographic components and thereby being less dependent on the starting model. Methods based on signal processing constitute adaptive filters proposed by Warner and Guasch (2014), Dynamic Image warping proposed by Ma and Hale (2013) or auxillary Bump Functional by Bharadwaj et al. (2016). Another proposed method is a hybrid optimization approach (Datta and Sen, 2016; Datta et al., 2016) where the starting model for FWI is estimated by using a combination of sparse parameterization in a global optimization method. Global methods are not strongly dependent on the choice of the starting model and because of sparse parameterization they converge in finite iterations. Once a starting model is estimated, it is used in the conventional FWI.

In this paper, we propose an extension to the velocity interface method to three dimensions. Following Datta and Sen (2016), we employ a sparse parameterization technique where we represent a velocity model using a set of interfaces and velocities across the interfaces. The idea behind our approach is to find an optimal set of interfaces and velocities in which the corresponding model has the minimum misfit using a global optimization technique. Once the model is estimated, we test it for correctness using the conventional FWI over a few 2D slices of the model.

THEORY

Consider a 3D velocity model defined by $v(x,y,z)$. We define a set of interfaces in 3D as $z_i(x,y)$, where z_i is the depth of the interface at (x,y). Each interface is in turn parameterized by a set of isodepth contours defined as point sets. The collection of pointsets are then interpolated to obtain interface defined in (x,y). 2 velocities v_{up} and v_{dn} are defined at the top and bottom of each interface. When the set of interfaces and the velocities across them are decided, the complete velocity model is built by linearly interpolating the velocities across them. This sparse parameterization allows us to represent a 3D model using a few finite parameters. To compute the seismic response of the models, we use the acoustic wave equation in 3D given by

$$\frac{1}{\mathbf{c}(x,y,z)^2}\frac{\partial^2 P}{\partial t^2} = \nabla^2 P + s(x,y,z,t)\,, \tag{1}$$

where $\mathbf{P}$ is the pressure wavefield, ∇^2 is the Laplacian given by $\frac{\partial^2}{\partial x^2}+\frac{\partial^2}{\partial z^2}+\frac{\partial^2}{\partial y^2}$, $\mathbf{c}(x,y,z)$ is the velocity field and $s(x,y,z,t)$ is the source term. We sample the pressure wavefield at the receiver locations to obtain the desired seismograms. The seismograms are then compared with the recorded seismograms using a cross-correlation objective function.

We find an optimal set of velocities and interfaces by minimizing the misfit between the data from the true 3D model and data from random models. We use Very Fast Simulated Annealing (VFSA) (Ingber and Rosen, 1992) for this purpose. A starting model is updated iteratively using a control parameter called temperature and unlike greedy algorithms, is able to accept worse solutions. A detailed overview of VFSA can be found in Sen and Stoffa (2013).

Using the VFSA derived model along several 2D slices, we carry out FWI. We use the same equation as in Equation 1. To compute the gradient we back propagate the data residuals using the adjoint state method (Plessix, 2006) given by

$$\frac{1}{\mathbf{c}(x,z)^2}\frac{\partial^2 R}{\partial t^2} = \nabla^2 R + \Delta\mathbf{d}\,(x,t)\,, \tag{2}$$

where $\mathbf{R}$ is the adjoint wavefield , and $\Delta\mathbf{d}\,(x,t)$ is the data-residual.

The gradient is computed by crosscorelating the forward wavefield with the adjoint one as

$$\frac{\partial E}{\partial \mathbf{m}} = \frac{1}{c\,(x,z)^3} \sum_{shots} \frac{\partial^2 P}{\partial^2 t} R. \tag{3}$$

The gradient is now used to update the model using a L-BFGS optimizer (Zhu et al., 1997) to obtain the final model update.

RESULTS

Validation test on toy model

First we demonstrate a proof of concept using a flat toy model with 4 layers and 3 interfaces shown in Figure 1. Because it is a model with flat interfaces, all shot gathers will give the same response. So we ran the inversion with just one shot in the center of the model. We ran the VFSA algorithm for 100 iterations to obtain an optimal set of interfaces and velocities. The true values of the depth of interfaces and the velocities, their search space and inverted values are show in Table 1. We observe that even with a wide search space we are able to obtain a model that is very close to the true model.

Toy model inversion			
	v_{up}	v_{dn}	Depth
Int 1	1500 [1500] (1500,1500)	2004 [2000] (1750,2250)	50 [50] (50,50)
Int 2	2009 [2000] (1700,2300)	2508 [2500] (2200,2800)	98 [100] (75,125)
Int 3	2520 [2500] (2200 2800)	3021 [3000] (2800,3500)	157 [150] (120,180)

Table 1: Table showing VFSA results for a 4-layered toy model with 3 interfaces. The true values are shown in square brackets and the search space is given in parentheses

SEG EAGE Overthrust Model

The second model we used was a modified EAGE-SEG 3D Overthrust model (Aminzadeh et al., 1997) shown in Figure 2(a). We selected half the grid points from the strike section making the model size (801,401,207) in the x, y and z directions respectively, each with a grid spacing of 15m. We generated synthetic data using a Ricker wavelet with a central frequency of 4Hz. The maximum offset were 9 km and 4.5 km in the dip and strike direction respectively. To obtain an initial guess for the interfaces, we heavily smoothed the model and extracted a few surfaces with the same velocities. For a real dataset, this can also be done after semblance based velocity analysis. We selected 5 interfaces from the smoothed model at velocity values between 2200 m/s and 6000m/s. From each interface a set of few points were identified. The search space of the few isodepths were put 500m top and below the initial isodepth. We ran VFSA for 100 iterations, the final model is shown in Figure 2(b). The error vs iteration plot is shown in Figure 3 . The curve shows that error oscillates in the initial iterations while in the later iterations it searches for a better solution in the vicinity of the current solution. To demonstrate the quality of inversion, we show the shot gathers from the true model vs the VFSA model in Figure 4. The gathers show that they do not suffer from cycle skipping and therefore, the derived model can potentially be a good starting model for standard FWI.

We took 2 slices from our 3D VFSA model from the (x,z) plane at y= 3km and 5.7km and performed a 2D FWI on both slices. The inversion was done at frequency ranges of 3,4,5,6 Hz for 30 iterations per frequency. The slices from the VFSA model are shown in Figure 5(b) and 6(b) while the final models are shown in Figures 5(c) and 6(c). The final model shows close resemblance to the true model shown in Figures 5(a) and 6(a) thereby demonstrating the effectiveness of the VFSA approach.

CONCLUSIONS

We present a novel FWI method using VFSA to estimate starting models in 3D. The method is largely automated and has the potential to automate velocity model building skipping on a few iterations of MVA. The algorithm is reliably able to estimate the correct set of interfaces and velocities the corresponding model of which gives the least misfit with the real data. The estimated models do not suffer from cycle skipping and is able to recover the true model after conventional FWI. The cost of this approach is comparable to standard FWI as it avoids extraneous forward modeling operations to compute gradient and step lengths.

ACKNOWLEDGMENTS

The authors are thankful to Hess Corporation for providing computational facilities and partial financial support.

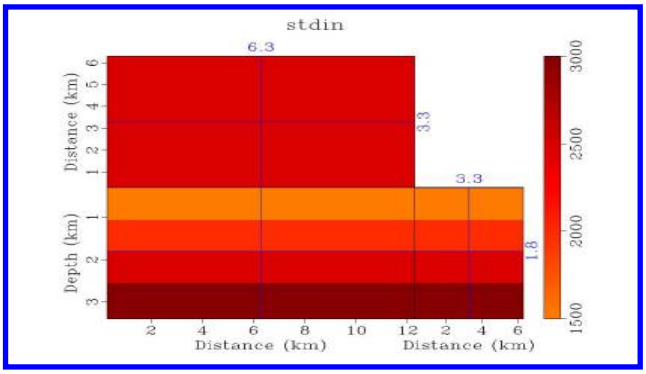

Figure 1: The 4 layer TOY model

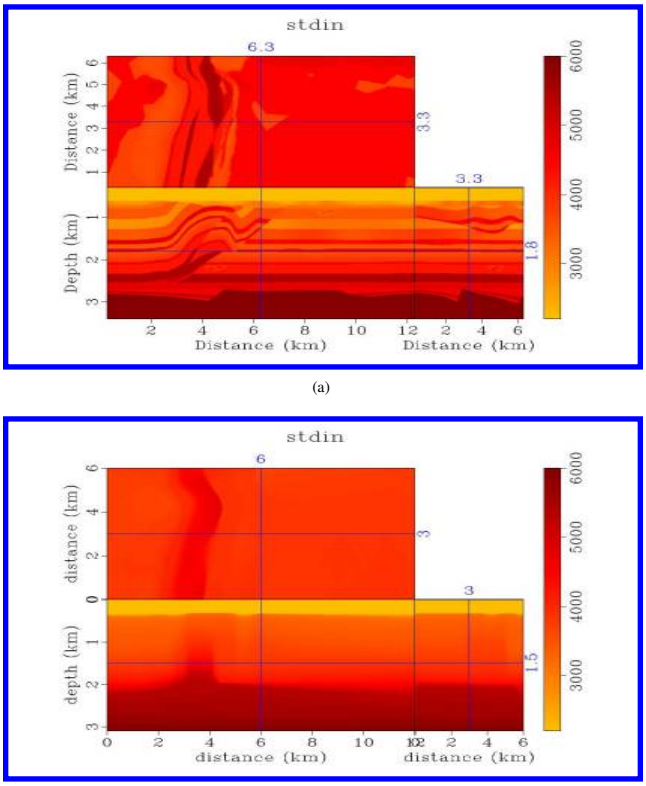

(a)

(b)

Figure 2: (a) True 2D SEG-EAGE Overthrust Model (b) Inverted model after VFSA

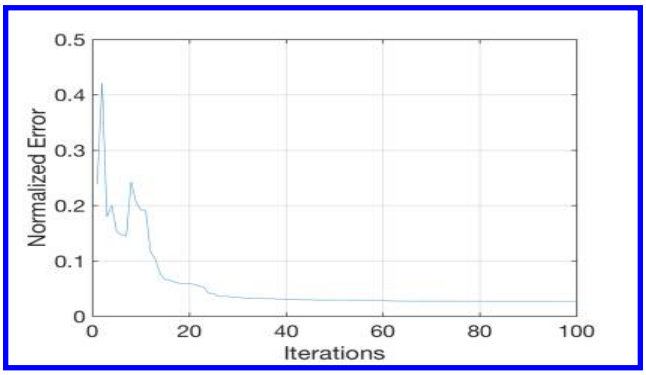

Figure 3: Error vs iterations for the SEG EAGE Overthrust Model

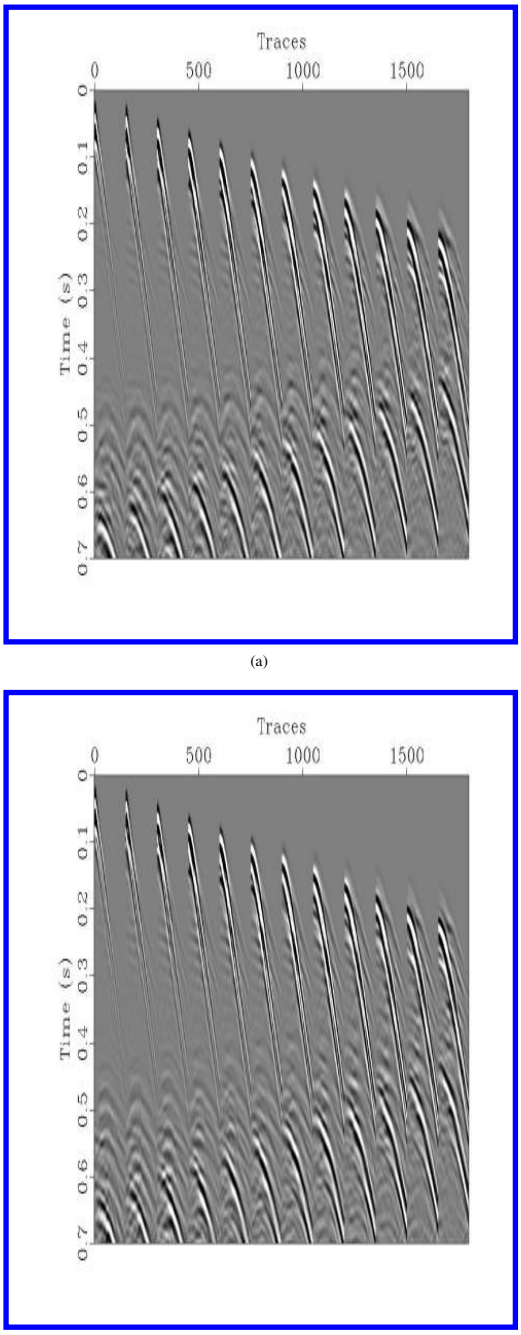

(a)

(b)

Figure 4: (a) Modelled Seismogram from the true SEG-EAGE overthrust model and (b) Modeled seismogram from the VFSA result

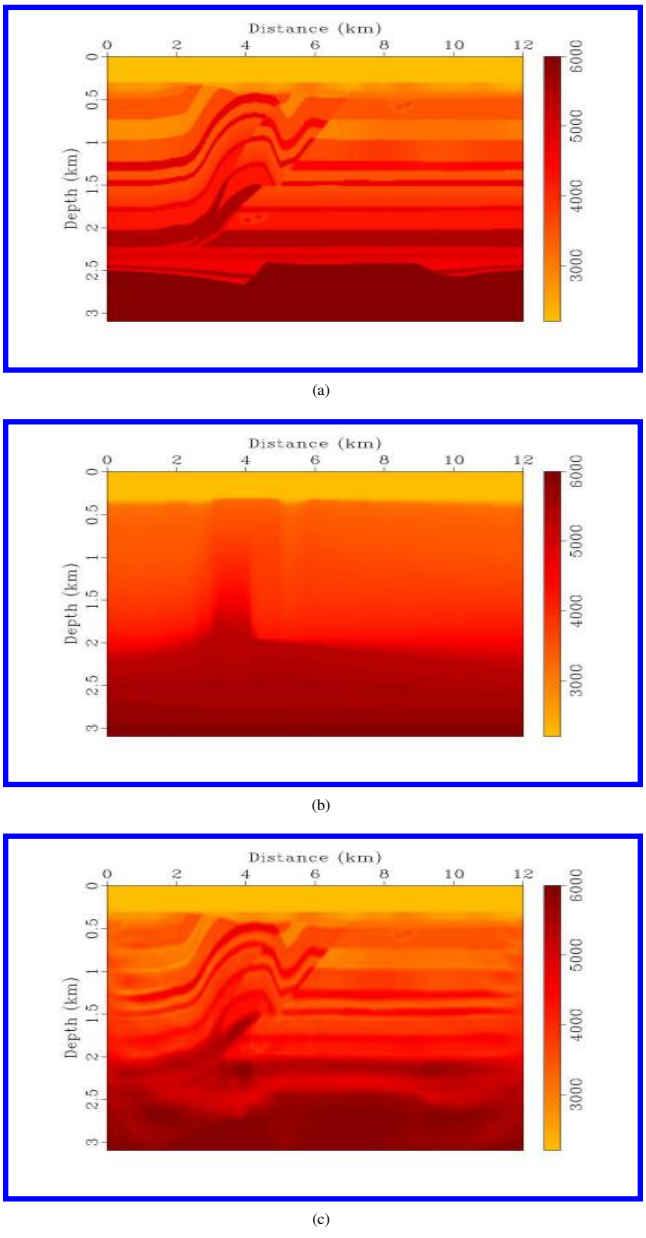

Figure 5: (a) The True 2D slice from the SEG-EAGE Overthrust Model (b) Starting slice from VFSA and (c) Inverted 2D model from (b)

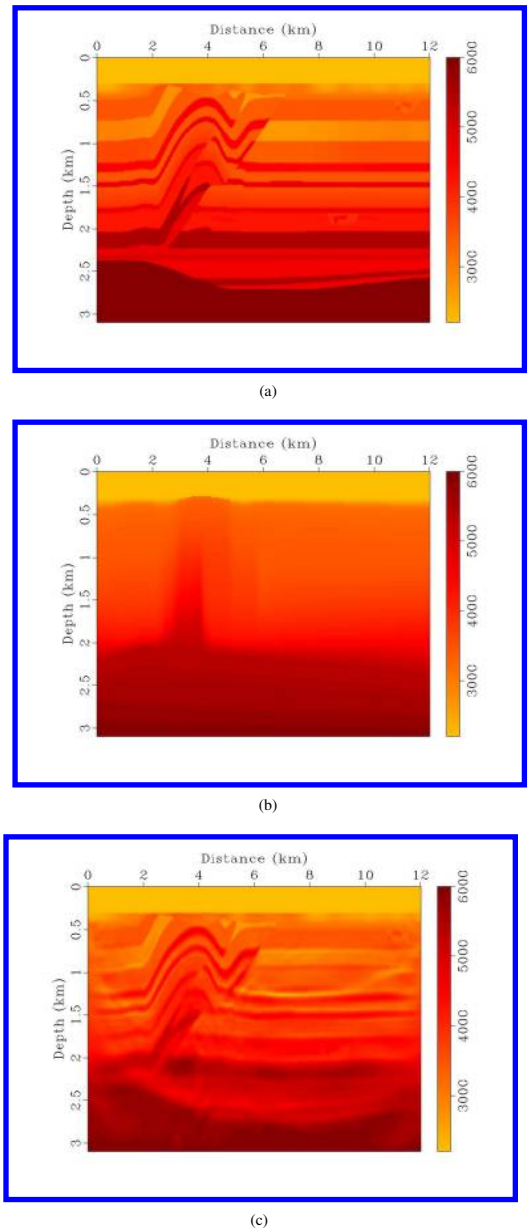

Figure 6: (a) The True 2D slice from the SEG-EAGE Overthrust Model (b) Starting slice from VFSA and (c) Inverted 2D model from (b)

EDITED REFERENCES

Note: This reference list is a copyedited version of the reference list submitted by the author. Reference lists for the 2017 SEG Technical Program Expanded Abstracts have been copyedited so that references provided with the online metadata for each paper will achieve a high degree of linking to cited sources that appear on the Web.

REFERENCES

Almomin, A., B. Biondi, 2012, Tomographic full waveform inversion: Practical and computationally feasible approach: 82nd Annual International Meeting, SEG, Expanded Abstracts, 1–5, https://doi.org/10.1190/segam2012-0976.1.

Aminzadeh, F., B. Jean, and T. Kunz, 1997, 3D salt and overthrust models: Society of Exploration Geophysicists.

Bharadwaj, P., W. Mulder, and G. Drijkoningen, 2016, Full waveform inversion with an auxiliary bump functional: Geophysical Journal International, **206**, 1076–1092, http://doi.org/10.1093/gji/ggw129.

Bunks, C., F. M. Saleck, S. Zaleski, and G. Chavent, 1995, Multiscale seismic waveform inversion: Geophysics, **60**, 1457–1473, http://doi.org/10.1190/1.1443880.

Datta, D., M. Sen, F. Liu, and S. Morton, 2016, Salt model building by shape-based parameterization and global FWI: 86th Annual International Meeting, SEG, Expanded Abstracts, 1069–1073, http://doi.org/10.1190/segam2016-13867592.1.

Datta, D., and M. K. Sen, 2016, Estimating a starting model for full-waveform inversion using a global optimization method: Geophysics, **81**, R211–R223, http://doi.org/10.1190/geo2015-0339.1.

Ingber, L., and B. Rosen, 1992, Genetic algorithms and very fast simulated reannealing: A comparison: Mathematical and Computer Modelling, **16**, 87–100, http://doi.org/10.1016/0895-7177(92)90108-W.

Kim, Y., C. Shin, H. Calandra, and D. J. Min, 2013, An algorithm for 3D acoustic time-Laplace-Fourier-domain hybrid full waveform inversion: Geophysics, **78**, R151–R166, http://doi.org/10.1190/geo2012-0155.1.

Ma, Y., and D. Hale, 2013, Wave-equation reflection traveltime inversion with dynamic warping and full waveform inversion: Geophysics, **78**, R223–R233, http://doi.org/10.1190/geo2013-0004.1.

Plessix, R.E., 2006, A review of the adjoint-state method for computing the gradient of a functional with geophysical applications: Geophysical Journal International, **167**, 495–503, http://doi.org/10.1111/j.1365-246X.2006.02978.x.

Sen, M. K., and P. L. Stoffa, 2013, Global optimization methods in geophysical inversion: Cambridge University Press, https://doi.org/10.1017/cbo9780511997570.

Sirgue, L., and R. G. Pratt, 2004, Efficient waveform inversion and imaging: A strategy for selecting temporal frequencies: Geophysics, **69**, 231–248, http://doi.org/10.1190/1.1649391.

Tarantola, A., 1984, Inversion of seismic reflection data in the acoustic approximation: Geophysics, **49**, 1259–1266, http://doi.org/10.1190/1.1441754.

Virieux, J., and S. Operto, 2009, An overview of full waveform inversion in exploration geophysics: Geophysics, **74**, WCC1–WCC26, http://doi.org/10.1190/1.3238367.

Warner, M., and L. Guasch, 2014, Adaptive waveform inversion: Theory: 84th Annual International Meeting, SEG, Expanded Abstracts, 1089–1093, http://doi.org/10.1190/geo2015-0387.1.

Zhu, C., R. H. Byrd, P. Lu, and J. Nocedal, 1997, Algorithm 778: Lbfgsb: Fortran subroutines for large-scale bound constrained optimization: ACM Transactions on Mathematical Software (TOMS), **23**, 550–560, http://doi.org/10.1145/279232.279236.